Synthesis and Characterization of New Carbazole Derivative for Photorefractive Materials

IONICA IONITA[1]*, ANA-MARIA ALBU [2,3], CRISTIANA RADULESCU[1]

[1]Valahia University of Targoviste, Faculty of Science and Arts, Department of Science, 18-24 Unirii Blv..,130082, Targoviste, Romania

[2] University Politehnica of Bucharest Department of Polymer Science, 149 Calea Victoriei, 010072, Bucharest, Romania

[3] Romanian Academy, Organic Chemistry Center Costin D. Nenitescu , 202B Spl. Independentei CP 35-108, 060023, Bucharest, Romania

The aim of the present study was to synthesize and characterize the new derivative with carbazole, such as (N,N-dimethyl-4-phenyl)-[3-[N-(2-hydroxyethyl)carbazolyl]]diazene (CzEtAzDMe) which can be used with success for the obtaining the new photorefractive materials. The synthesis of this compound : carbazole derivative was achieved by diazotization of 4-amino-N,N-dimethylaniline with $NaNO_2$ and H_2SO_4 and coupling the obtained diazonium salt with N-(2-hydroxyethyl)-carbazole. In order to establish the chemical structure of the new compound, the organic intermediate as well as CzEtAzDMe was purified by HPTLC. The purified compounds were characterized by spectral analysis (FTIR, UV-Vis) and Differential Scanning Calorimetry (DSC). Quartz crystal microbalances (QCM) technique was used in order to monitor the physical properties associated to the surface and interfacial processes of synthesized carbazole derivative.

Keywords: carbazole, (N,N-dimethyl-4-phenyl)-[3-[N-(2-hydroxyethyl)carbazolyl]]diazene, photorefractive, spectral analysis, DSC, Quartz Crystal Microbalance.

In the last years the aromatic azo polymers have been widely used due to their application in different optical fields [1]. After the photorefractive effect of organic compounds was discovered, several polymers which containing carbazole have become attractive from the point of view of their photoconductivity [2, 3]. The photoconductive and electro-optic functionalities in the side-chain of those polymers can be considered as potential materials for photorefractive applications. Therefore the azobenzene photochemistry continue to produce unexpected phenomena because the azobenzene group is incorporated into the polymer, and in this respect the photoisomerization phenomenon can have unexpected possible consequences [4]. It is well known that in the polymer materials with carbazole can appear the possibility of building several variable spacers between the azo group and the main chain which can increase the order degrees as well as the azo group becomes much decoupled from the main-chain motion.

Photoconductive films based on poly-*N*-vinylcarbazole derivates are widely used as media for recording and modulation of optical radiation. Molecules of organic additions contained in the above-indicated films serve as centres of light absorption and photogeneration of charge carriers.

The photorefractive polymers with carbazole ring and azo moieties in the side chain have all the necessary elements for photorefractivity properties (electro-optic chromophore and charge trappers). The azo-containing carbazole groups provided both the photoconductivity and non-linear optical (NLO) activity, and the aliphatic chain attached on the nitrogen atom of the carbazole ring acts as spacer [5]. Hence, the photorefractive polymers exhibit equally photoconductivity and optical nonlinearity. They have concerned substantial interest due to their potential applications in optical computing, optical correlation, 3D data or image storage. Large parts of the reported fully functionalized photorefractive polymers are prepared by applying of a backbone functionalized with separate charge generator, charge transporter, and non-linear optical (NLO) chromophore. The NLO chromophore and the charge transporting component compete for volume fraction in the photorefractive polymers as well [6].

The aim of this research was the synthesis and characterization (FTIR, UV-Vis, and DSC) of new carbazole derivative substituted with chromophore azo group [7] which can be used with success as basic material of photorefractive polymers. All synthesized compounds were purified by HPTLC. The physical properties associated to the surface and interfacial processes of synthesized carbazole derivative were performed by the Quartz Crystal Microbalance (QCM) technique.

Experimental part

Reagents and synthesis

All materials (i.e. 4-amino-*N,N*-dimethylaniline, carbazole, sodium dodecyl benzenesulfonate, 2-bromethanol, DMF, $NaNO_2$, H_2SO_4, CH_2Cl_2, and KOH) used in synthesis procedure of photorefractive derivatives with carbazole were acquired from Aldrich, and have high purities.

The synthesis of carbazole derivative can be achieved by following steps: (1) the diazotization of 4-amino-*N,N*-dimethylaniline with $NaNO_2$ and H_2SO_4 at -4°C, when the diazonium salt was obtained; (2) the coupling diazonium salt with *N*-(2-hydroxyethyl)-carbazole when the (*N,N*-dimethyl-4-phenyl)-[3-[*N*-(2-hydroxyethyl) carbazolyl]]diazene compound was synthesized [8].

This reaction was performed in two steps as well: *N*-(2-hydroxyethyl)-carbazole was dissolved in CH_2Cl_2 and then

* email: ioana67@gmail.com

sodium dodecyl benzenesulfonate (NaDBS) was added. The obtained mixture was stirred 24 h at room temperature. Finally, *N,N*-dimethyl-4-phenyl)-[3-[*N*-(2-hydroxyethyl) carbazolyl]]diazene [CzEtAzDMe] was obtained (scheme 1) which was dissolved in C_2H_5OH and distilled to remove all CH_2Cl_2. The red-brown obtained precipitate was filtered, washed with water and dried in air and CzEtAzDMe purified by HPTLC.

The *N*-(2-hydroxyethyl)-carbazole coupling component was synthesized by carbazole alkylation in presence of KOH, like as: carbazole was dissolved in DMF for 45 min and then 2-bromethanol was added very slowly, under stirring at 20°C, in 10 h. Then the final product was precipitated in water, when is obtained white "cotton" which was filtrated and dried in air.

The *N*-(2-hydroxyethyl)-carbazole intermediate used in coupling reaction (scheme 1) was purified by High Performance Thin Layer Chromatography (HPTLC) by using a semiautomatic spotting system Linomat 5 (Camag), TLC densitometer Scanner 3 (Camag, Switzerland) using WinCATS software. (*N,N*-Dimethyl-4-phenyl)-[3-[*N*-(2-hydroxy-ethyl)carbazolyl]]diazene compound was purified by HPTLC as well, by using the same device from Camag, Switzerland.

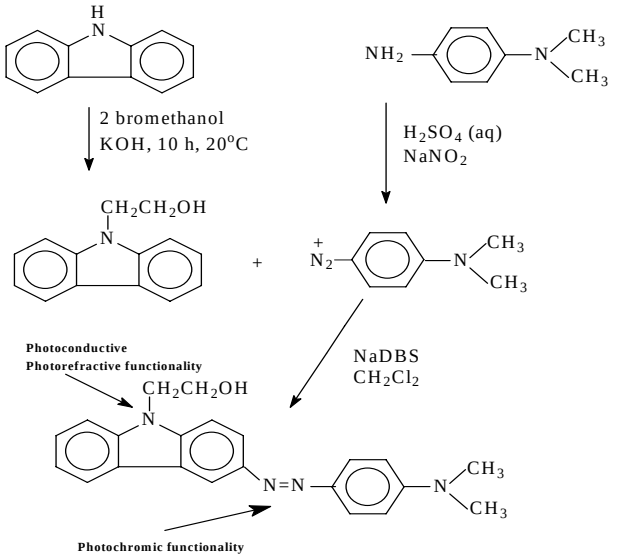

(*N,N*-dimethyl-4phenyl)-[3-[*N*-(2 hydroxyethyl)carbazolyl]]diazene

Scheme 1. Chemical structure of photorefractive derivative with carbazole (CzEtAzDMe)

In order to obtain compounds with high purity the HPTLC method was chosen, especially due several advantages: repetition of densitometric evaluation of the same sample can be achieved under different conditions without repeating the chromatography to optimize quantification, since all sample fractions are stored on the HPTLC plate; ability to choose solvents for the mobile phase is not restricted by low UV transparency or the need for ultra-high purity; high sample throughput since several samples can be chromatographed simultaneously; accuracy and precision of quantification is high because samples and standards are chromatographed and measured under the identical experimental conditions on a single HPTLC plate.

Structural characterization and analyses

The chemical structure of obtained compound was characterised by FTIR spectroscopy by using a Bruker Vertex 70 spectrometer equipped with an attenuated total reflection (ATR) accessory with a diamond crystal.

In order to obtain more usefully information about the chemical structure of CzEtAzDMe, the UV-Vis investigation was performed by using an SPECORD M400 Carl Zeiss Jena double-beam and a monochromator spectrophotometer. The sample was dissolved in ethanol at room temperature.

The thermal properties were achieved by Differential Scanning Calorimetry (DSC) and by using a Setram 131 Evo (Setaram Instrumentation, Caluire, France) in either inert (nitrogen) or oxidant (air) atmosphere at a constant heating rate (10°/min). The gas (nitrogen or air) flow rate was 50 mL/min, and the temperature range was 25 – 650°C (for the measurements in nitrogen atmosphere) or 25 – 450°C (for the measurements in air atmosphere). The weight of the DSC samples was 12 – 15 mg (powdered material). The DSC measurements were performed in either alumina (for the measurements in nitrogen, up to 650°C) or aluminium crucibles (for the measurements in air, up to 450°C). The oxidation induction temperature has been determined according to reference standards [9, 10] as the temperature corresponding to the oxidation process onset.

In order to study a wider number of physical and chemical properties associated to the surface and interfacial processes of synthesized carbazole derivative which can lead to a higher reliability of the study results a Quartz Crystal Microbalance (QCM) technique was chosen.

The benefit of the QCM technique is that it allows for a label free detection of molecules. This is a result of the fact that the frequency response of the quartz resonator is proportional to the raise in thickness of the adsorbed layer. QCM has many advantages over the traditional sensing methods such as high sensitivity (up to $\mu g/cm^2$ to ng level), non-invasiveness, long-term measurements, and free labels. It has a wide detection range from a monolayer of small molecules to much greater masses-even complex arrays of whole cells. The analysis was performed with a QCM200 (Stanford Research Systems) equipped with a controller and oscillator QCM25, crystal support, flow cell, peristaltic pump, and SRFQCM200 software, under LabView, as well. The used standard sensor crystal consists, using a thin disk at 5-15 MHz resonant frequency, AT-cut, α-quartz with circular electrodes patterned on both sides.

Results and discussions

In order to be purified, the synthesized compounds (i.e. *N*-(2-hydroxyethyl)-carbazole and (*N,N*-dimethyl-4-phenyl)-[3-[*N*-(2-hydroxyethyl)carbazolyl]]diazene) were spotted separately in lines under nitrogen flow on silicagel 60 F254 Merck pre-coated plates, and the mobile phase identified as giving optimum performance being the mixture acetic acid: ethanol: water (1:4:1). The plates were analysed by densitometry at 254 nm, and the obtained R_f for *N*-(2-hydroxyethyl)-carbazole. The coupling compound was 0.81 ±0.01 and for CzEtAzDMe it was 0.84 ±0.01. The semi-quantitative assay leads to a linear regression when using the peak maximum and the peak area, with correlation coefficients over 0.99.

(*N,N*-dimethyl-4-phenyl)-[3-[*N*-(2-hydroxyethyl) carbazolyl]]diazene and the intermediary *N*-(2-hydroxyethyl)-carbazole was obtained with good yields such as 84.7% and 92.2% respectively.

The chemical structure of the novel compound *N,N*-dimethyl-4-phenyl)-[3-[*N*-(2-hydroxyethyl)carbazolyl]] diazene (CzEtAzDMe) was investigated by FTIR spectroscopy. The FTIR spectra (fig. 1) proved the transformation of carbazole (Cz) in CzEtAzDMe by decreasing the signal 3413 cm^{-1} for ν_{NH} as well as a wide

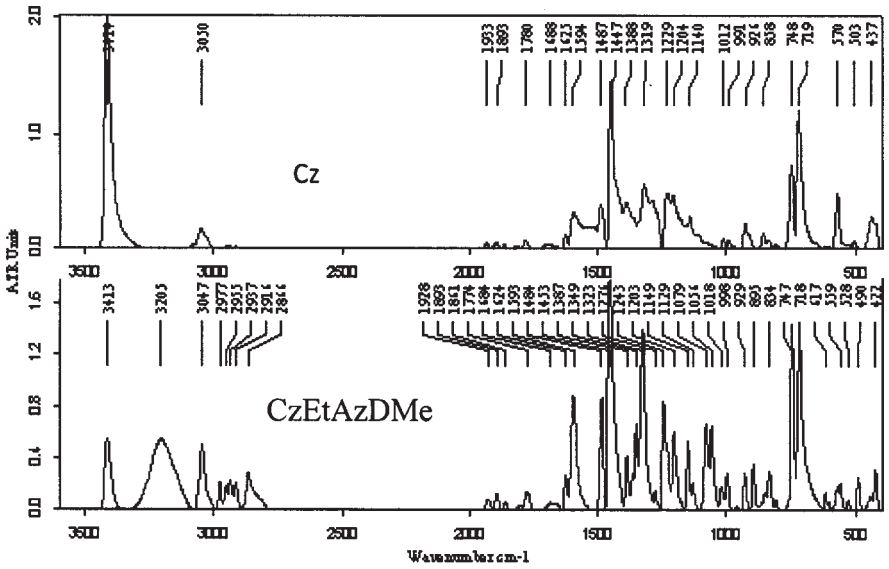

Fig. 1. FTIR spectra of Cz and CzEtAzDMe

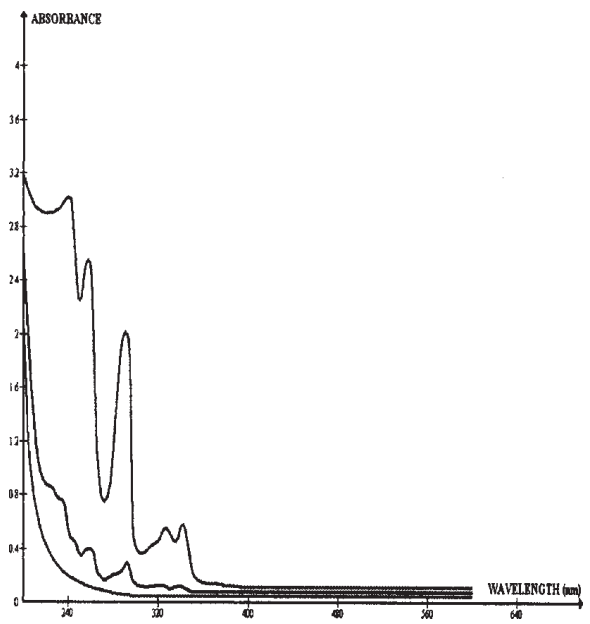

N-(2-hydroxyethyl)carbazole

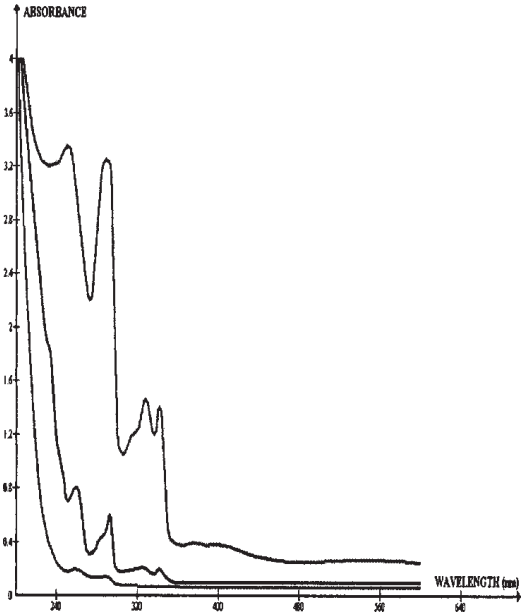

(*N,N* dimethyl-4phenyl)-[3-[*N*-(2-hydroxyethyl)carbazolyl]]diazene

Fig. 2. UV-Vis absorption spectra in ethanol

band which appear at 3205 cm^{-1}, characteristic signal of ν_{OH}. The other relevant signals are situated at 3047 cm^{-1} (aromatic stretching vibration); 2977 cm^{-1} for ν_{sym} corresponding to C–H of $N(CH_3)_2$; 2937- 2866 cm^{-1} stretching vibration of alkyl sequence; 1593 cm^{-1} ($\nu_{C=C}$ aromatic) 895 and 834 cm^{-1} (δ_{CH} substituted aromatic ring 1,4); 2977 - 2866 cm^{-1} (ν_{CH} aliphatic).

The UV-Vis spectra (fig. 2) show either three or five clear absorption bands, with maximum wavelength 240, 260, 290, 330, and 345, nm for the *N*-(2-hydroxyethyl)carbazole and 260, 290, 335, 350 and 400 nm for the (*N,N*-dimethyl-4-phenyl)-[3-[*N*-(2-hydroxyethyl)carbazolyl]]diazene, depending on the concentration (i.e. both analysed compounds were prepared in ethanol with concentration of the following: $2 \cdot 10^{-4}$ mol/L – violet spectrum, $2 \cdot 10^{-5}$ mol/L – blue spectrum and $2 \cdot 10^{-6}$ mol/L – green spectrum).

The absorption bands at a wavelength of over 300 nm were attributed to the combined electronic transitions such as n–π*, π–π* and internal charge transfer of the azoaromatic chromophore. The other, smaller signals used at a different wavelength, are recognized for the sum of several contributions due to the π–π* electronic transition of the di-/tri- substituted aromatic ring and the π–π* electronic transitions of carbazole chromophore.

The thermal investigation, showed in the fig. 3, reveal the specific comportment of such materials. Analysing the DSC diagrams for the three products we notice a simplification of thermal evolution in the same time with increasing the molecular structure. Thus, for the starting amine (fig. 3a) the thermal modifications records five endothermic peaks and three exothermic peaks respectively. The hydroxyl derivate of carbazole (fig. 3b) is characterized for endothermic peaks and a single exothermic peak, whereas for the final product we have only a broad exothermic and endothermic peak, shifted at superior temperatures.

Generally, in DSC measurements, all exothermic peaks showed a chemical reaction, as the endothermic peaks denote a physical organization for the low thermal interval, as well as a melting of the analysed substance.

In our case for the amine (fig. 3a) the alternation of the endothermic and exothermic peaks underline a progressive degradation process, mainly due to the decomposition of the amine, followed by the molecular reorganization (endothermic peaks). Only for the last peaks situated at 303°C we can talk about a real melting process: the broad

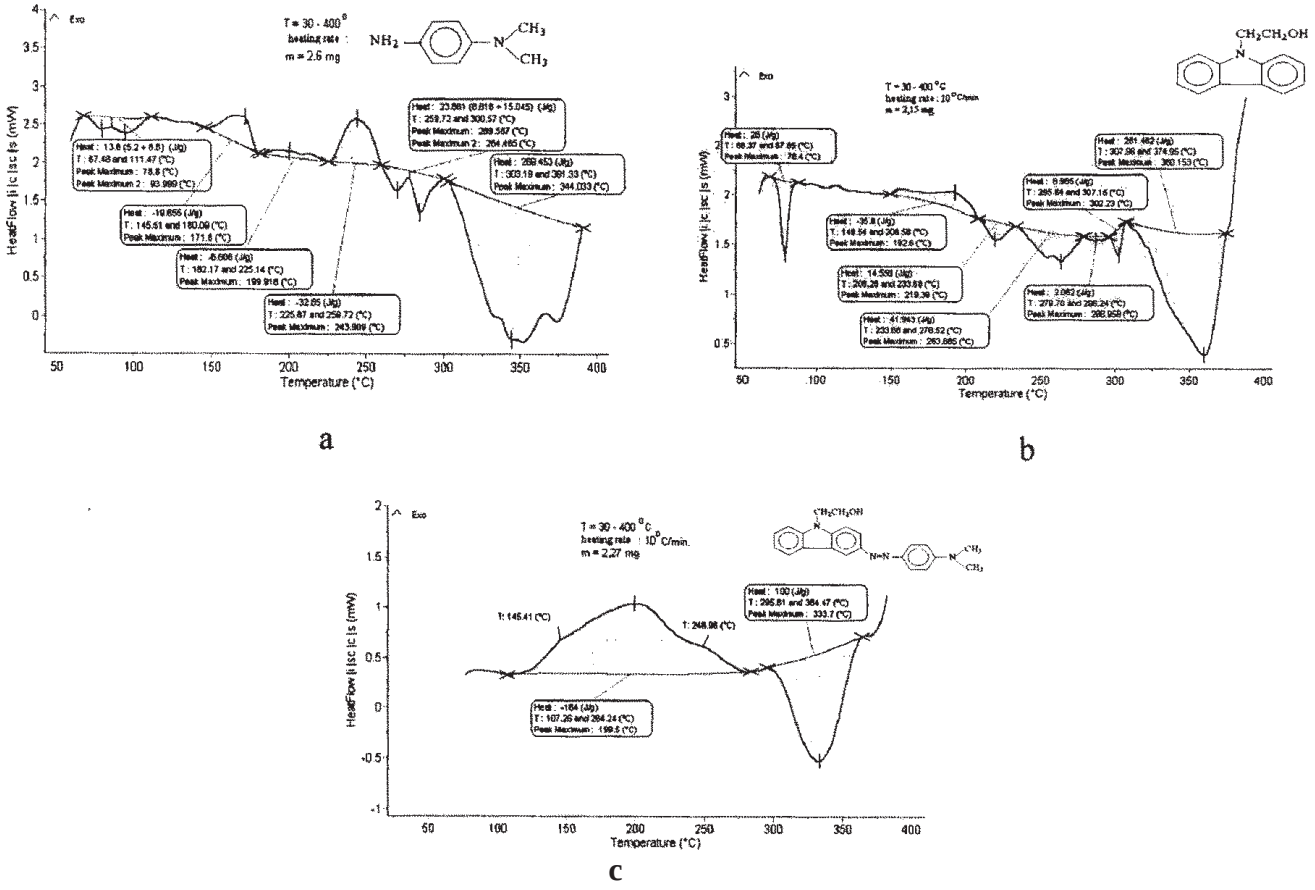

Fig.3. The DSC curves for 4-amino-*N,N*-dimethylaniline (a), *N*-(2-hydroxyethyl)carbazole (b) and (*N,N*-dimethyl-4-phenyl)-[3-[N-(2-hydroxyethyl)carbazolyl]]diazene (c)

peaks and the reaction heat are very high by comparison to the other anterior signals.

Similarly can be said for the hydroxyl ethyl carbazole (fig. 3b). In this case the only exothermic peak, with a maximum at 192.6°C is the etherification consequence. The following series of the three endothermic peaks is justified by the different dimensional ether compounds. Such as, the real melting point is recorded at 286.95°C.

More unitary is the azo compound: in this case the exothermic peak at 199.5°C is probably due to the presence of the low molecular impurities; their melting point has recorded at 333.7°C.

Quartz Crystal Microbalance (QCM) has found numerous applications in many fields including thin-film measurement, chemical analysis, gas sensor, humidity sensor and biosensor [11]. Especially, the development of QCM systems for the use in fluids or with viscoelastic deposits has dramatically increased the interest towards this technique [11-13]. The quartz crystal microbalance is an extremely sensitive sensor capable to measure the mass changes in the ng/cm^2 range with a wide dynamic range extending into the 100 μg/cm^2 range [14, 15]. The sensibility depends on the detector area and the type of solid electrode in contact with the fluids [16, 17].

In this research Quartz Crystal Microbalance was used to monitor in real-time the (*N,N*-dimethyl-4-phenyl)-[3-[*N*-(2-hydroxy-ethyl)carbazolyl]]diazene adsorption followed by *N*-(2-hydroxyethyl)carbazole adsorption and as well as optimization of interaction processes and determination of solution effects on the analytical signal. Solutions of (*N,N*-dimethyl-4-phenyl)-[3-[*N*-(2-hydroxyethyl) carbazolyl]]diazene in ethanol are adsorbed on a gold electrode (e.g. CrAu electrode) of QCM and the sensor response are estimated through decrease of the QCM frequency.

In addition, the response of the sensor at *N*-(2-hydroxyethyl) carbazole in ethanol is rapid, large, and reversible. A well-established volume of analysed samples (e.g. 0.5 mL) was deposited on the electrode surface and the frequency (F) and the resonance (R) were calculated. The analyses were achieved on three electrodes such as: chromium/gold, titanium/gold, and titanium/platinum with a 1 inch diameter for each electrode. It was observed that only the response of chromium/gold electrode at absorption of *N*-(2-hydroxyethyl)carbazole and (*N,N*-dimethyl-4-phenyl)-[3-[*N*-(2-hydroxyethyl)carbazolyl]]diazene respectively, was estimated through decrease of QCM frequency. Therefore the resonant frequency changes as a linear function of the mass of substance deposited on the crystal surface. The resistance of sensor was analyzed at approximately every 5 s. Hence, the resistance at resonance modifications with the viscosity of the solutions in connection with the crystal surface was calculated as well.

The SRFQCM200 software, under LabView, shown the variation in time of these two parameters and recorded the measured values of calculated parameters (ΔF, ΔR) depending on the concentration (i.e. 2 . 10^{-4} mol/L, 2 . 10^{-5} mol/L and 2 . 10^{-6} mol/L for *N*-(2-hydroxyethyl)carbazole and (*N,N*-dimethyl-4-phenyl)-[3-[*N*-(2-hydroxyethyl) carbazolyl]]diazene, respectively (fig. 4 - 7). The sensor response to each component exposure was DR - the maximum resistance modify noticed during exposure to the component. DR data were considered by subtracting from all records points a straight line fit to the basic exposure. It has been exposed to increase linearly with the concentration of the each solution. From the figure 4-7 we can conclude that the ethanol, which is the polar solvent, did not influence the adsorption in real-time of the molecules of the synthesized compounds and implicitly

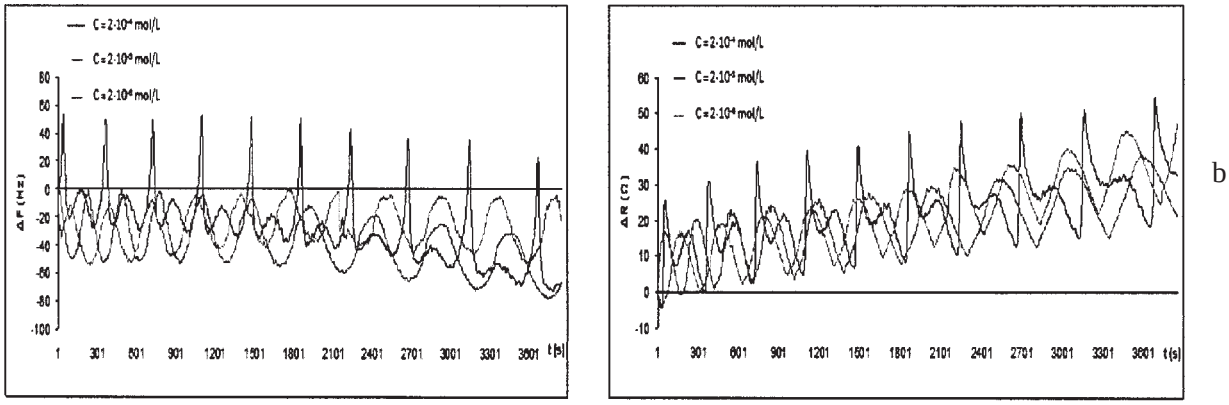

Fig. 4. (a) Frequency shift (Hz) and (b) resistance shift (Ohms) versus time with QCM static of *N*-(2-hydroxyethyl) carbazole in ethanol at different concentration

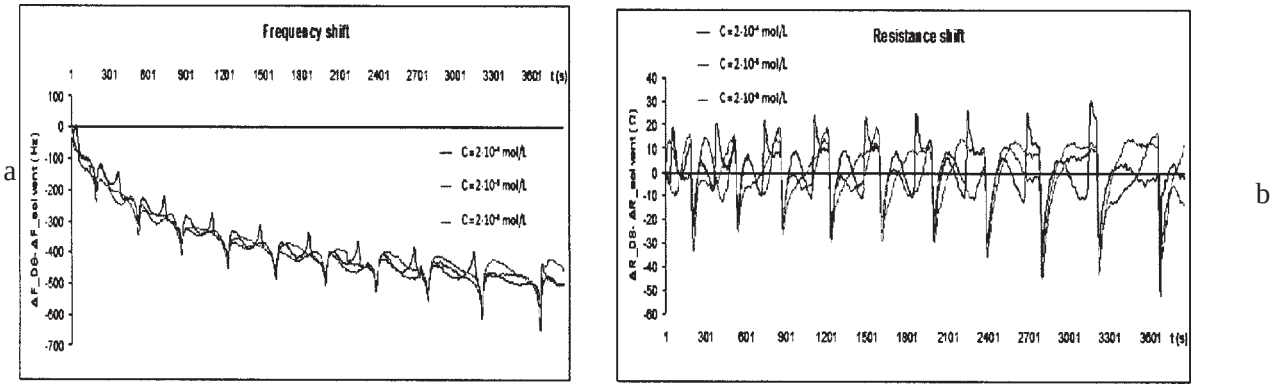

Fig. 5. (a) Frequency shift (Hz) and (b) resistance shift (Ohms) versus time with QCM static of *N*-(2-hydroxyethyl) carbazole without ethanol at different concentration

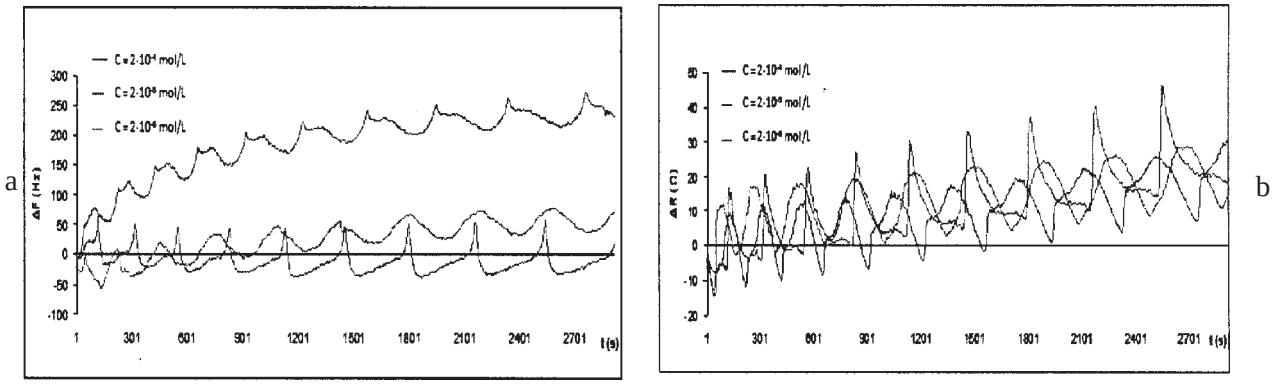

Fig. 6. (a) Frequency shift (Hz) and (b) resistance shift (Ohms) versus time with QCM static in *(N,N*-dimethyl-4-phenyl)-[3-[*N*-(2-hydroxyethyl)carbazolyl]]diazene in ethanol at $2 \cdot 10^{-4}$ mol/L, $2 \cdot 10^{-5}$ mol/L and $2 \cdot 10^{-6}$ mol/L

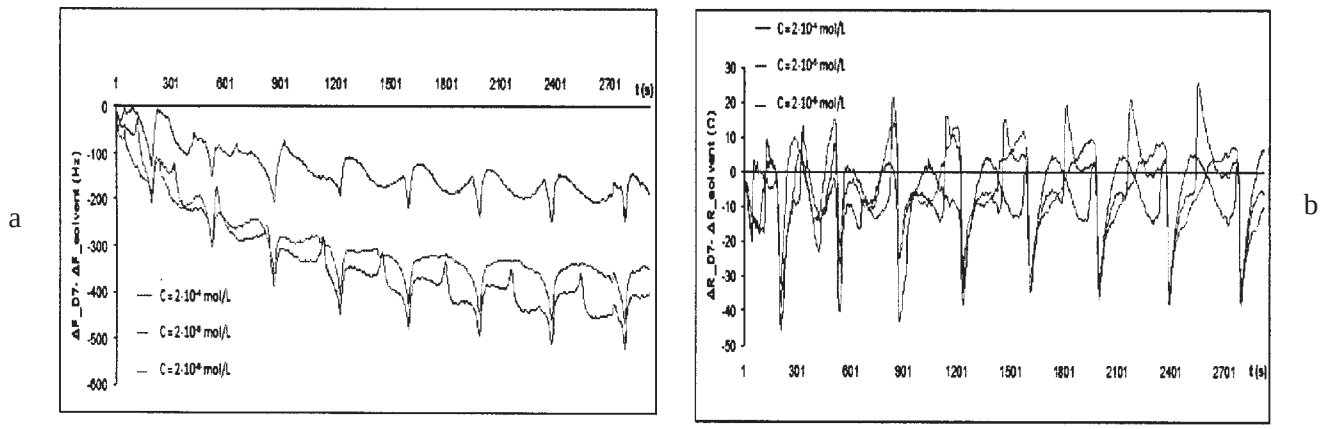

Fig. 7. (a) Frequency shift (Hz) and (b) resistance shift (Ohms) versus time with QCM static in *(N,N*-dimethyl-4-phenyl)-[3-[*N*-(2-hydroxyethyl)carbazolyl]]diazene without ethanol at $2 \cdot 10^{-4}$ mol/L, $2 \cdot 10^{-5}$ mol/L and $2 \cdot 10^{-6}$ mol/L

the response of the sensor. After 1 h the ethanol was evaporated and on the sensor remained only the *N*-(2-hydroxyethyl)carbazole and (*N*,*N*-dimethyl-4-phenyl)-[3-[*N*-(2-hydroxyethyl) carbazolyl]]diazene respectively.

Therefore the mass of the organic compounds (i.e. *N*-(2-hydroxyethyl)carbazole and (*N*,*N*-dimethyl-4-phenyl)-[3-[*N*-(2-hydroxyethyl)carbazolyl]]diazene) adsorbed on the sensor leading a shift in the frequency of the QCM crystal ΔF, changes of resonant frequency of the crystal can be referenced to changes in mass through the Sauerbrey equation (1.1). This allows determination of the each compound mass absorbed per unit mass of the deposited compound (table 1 and 2).

$$\Delta F = \frac{-2f_0^2}{A\sqrt{\rho_q \cdot \mu_q}} \cdot \Delta m \quad (1.1)$$

where ΔF is the change in resonant frequency (Hz) upon exposure to the analyte of interest, F_0 is the initial resonant frequency of the crystal (Hz), Δm is the change in mass (g), A is the piezoelectrically active area of the crystal (cm^2), ρ_q is the density of quartz (g/cm^3), and μ_q is the shear modulus of quartz (GPa).
where:

Table 1
FREQUENCY, RESISTANCE AND MASS VARIATION DEPENDING ON TIME FOR *N*-(2-HYDROXYETHYL)CARBAZOLE AT DIFFERENT CONCENTRATIONS

	Δt [s]	$\overline{\Delta F}$ [Hz]	$\overline{\Delta R}$ [Ω]	$\overline{\Delta F} - \overline{\Delta F_0}$ [Hz]	$\overline{\Delta R} - \overline{\Delta R_0}$ [Ω]	Δm [μg/cm²]
N-(2-hydroxyethyl)carbazole [$2 \cdot 10^{-4}$ mol/L]	0-300	-0.072	0.021	-0.601	0.004	0.01062
	301-600	-0.153	0.081	-1.441	0.023	0.02547
	601-900	-0.119	0.123	-1.796	-0.008	0.03173
	901-1200	-0.116	0.119	-2.233	0.006	0.03945
	1201-1500	-0.161	0.177	-2.564	0.097	0.04531
	1501-1800	-0.170	0.158	-2.653	0.045	0.04688
	1801-2100	-0.213	0.120	-2.782	0.001	0.04915
	2101-2400	-0.242	0.163	-2.884	-0.058	0.05096
	2401-2700	-0.238	0.222	-2.977	-0.013	0.05259
	2701-3000	-0.315	0.225	-3.123	0.057	0.05518
	3001-3300	-0.375	0.186	-3.168	-0.011	0.05597
	3301-3600	-0.380	0.171	-3.227	-0.015	0.05701
N-(2-hydroxyethyl)carbazole [$2 \cdot 10^{-5}$ mol/L]	0-300	-0.127	0.067	-0.656	0.050	0.01158
	301-600	-0.294	0.126	-1.582	0.068	0.02796
	601-900	-0.322	0.125	-1.998	-0.007	0.03530
	901-1200	-0.274	0.153	-2.391	0.040	0.04224
	1201-1500	-0.147	0.154	-2.551	0.075	0.04506
	1501-1800	-0.152	0.096	-2.636	-0.018	0.04657
	1801-2100	-0.293	0.115	-2.862	-0.004	0.05057
	2101-2400	-0.237	0.152	-2.879	-0.069	0.05087
	2401-2700	-0.276	0.135	-3.015	-0.100	0.05326
	2701-3000	-0.326	0.179	-3.133	0.010	0.05536
	3001-3300	-0.320	0.169	-3.113	-0.027	0.05500
	3301-3600	-0.399	0.185	-3.247	-0.001	0.05736
N-(2-hydroxyethyl)carbazole [$2 \cdot 10^{-6}$ mol/L]	0-300	-0.145	0.005	-0.674	-0.013	0.01191
	301-600	-0.293	0.023	-1.581	-0.035	0.02794
	601-900	-0.306	0.057	-1.982	-0.074	0.03502
	901-1200	-0.289	0.104	-2.405	-0.009	0.04250
	1201-1500	-0.224	0.152	-2.628	0.072	0.04643
	1501-1800	-0.109	0.169	-2.593	0.056	0.04581
	1801-2100	-0.044	0.141	-2.613	0.022	0.04616
	2101-2400	-0.131	0.115	-2.773	-0.106	0.04899
	2401-2700	-0.251	0.163	-2.990	-0.072	0.05283
	2701-3000	-0.199	0.235	-3.007	0.066	0.05312
	3001-3300	-0.094	0.212	-2.887	0.016	0.05100
	3301-3600	-0.214	0.205	-3.061	0.019	0.05408

Table 2

FREQUENCY, RESISTANCE AND MASS VARIATION DEPENDING ON TIME FOR (*N,N*-DIMETHYL-4-PHENYL)-[3-[*N*-(2-HYDROXYETHYL)CARBAZOLYL]]DIAZENE (CzEtAzDMe) AT DIFFERENT CONCENTRATIONS

	Δt [s]	$\overline{\Delta F}$ [Hz]	$\overline{\Delta R}$ [Ω]	$\overline{\Delta F} - \overline{\Delta F_0}$ [Hz]	$\overline{\Delta R} - \overline{\Delta R_0}$ [Ω]	Δm [μg/cm^2]
CzEtAzDMe [2·10^{-4} mol/L]	0-300	0.054	-0.012	-0.475	-0.030	0.00839
	301-600	-0.035	0.030	-1.323	-0.028	0.02338
	601-900	-0.190	0.080	-1.867	-0.051	0.03298
	901-1200	-0.218	0.087	-2.334	-0.026	0.04124
	1201-1500	-0.225	0.127	-2.629	0.047	0.04645
	1501-1800	0.051	0.169	-2.432	0.056	0.04297
	1801-2100	0.134	0.140	-2.435	0.021	0.04303
	2101-2400	-0.060	0.093	-2.702	-0.128	0.04774
	2401-2700	-0.142	0.131	-2.881	-0.105	0.05090
	2701-3000	-0.194	0.206	-3.001	0.037	0.05303
	3001-3300	-0.112	0.207	-2.904	0.010	0.05131
	3301-3600	-0.089	0.184	-2.936	-0.002	0.05187
CzEtAzDMe [2·10^{-5} mol/L]	0-300	0.385	0.028	-0.144	0.010	0.00254
	301-600	0.805	0.038	-0.484	-0.020	0.00855
	601-900	1.018	-0.012	-0.658	-0.144	0.01163
	901-1200	1.242	-0.031	-0.874	-0.144	0.01544
	1201-1500	1.289	0.005	-1.115	-0.074	0.01969
	1501-1800	1.317	0.071	-1.166	-0.042	0.02061
	1801-2100	1.445	0.124	-1.124	0.005	0.01986
	2101-2400	1.583	0.132	-1.059	-0.089	0.01872
	2401-2700	1.573	0.097	-1.166	-0.138	0.02060
	2701-3000	0.759	0.036	-2.049	-0.133	0.03620
	3001-3300	0.000	0.000	-2.793	-0.197	0.04934
	3301-3600	0.000	0.000	-2.847	-0.186	0.05031
CzEtAzDMe [2·10^{-6} mol/L]	0-300	-0.128	0.047	-0.657	0.030	0.01161
	301-600	-0.188	0.076	-1.477	0.018	0.02609
	601-900	-0.077	0.078	-1.753	-0.054	0.03097
	901-1200	0.020	0.115	-2.096	0.002	0.03703
	1201-1500	0.162	0.144	-2.242	0.064	0.03961
	1501-1800	0.343	0.124	-2.140	0.011	0.03782
	1801-2100	0.407	0.073	-2.162	-0.046	0.03819
	2101-2400	0.299	0.084	-2.343	-0.137	0.04140
	2401-2700	0.279	0.153	-2.460	-0.082	0.04346
	2701-3000	0.440	0.174	-2.367	0.006	0.04183
	3001-3300	0.484	0.126	-2.308	-0.070	0.04078
	3301-3600	0.338	0.151	-2.509	-0.035	0.04433

Δt - time interval [s];

ΔF - frequency variation media of analyzed compound in ethanol depending on time [Hz];

ΔR - resistance variation media of analyzed compound in ethanol depending on time [Ω];

ΔF_o - frequency variation media of ethanol in time [Hz];

ΔR_o - resistance variation media of ethanol in time [Ω];

Δm - mass variation for each analyzed compound in time [μg/cm^2].

However, very few effects were seen (fig. 4-7 and table 1-2) correlated to chain length differences and molecular mass which is 358 for (*N,N*-dimethyl-4-phenyl)-[3-[*N*-(2-hydroxyethyl)carbazolyl]]diazene so higher comparative with 211 for *N*-(2-hydroxyethyl)carbazole. One notable difference between the two compounds is the higher accessibility of the azo group in new (*N,N*-dimethyl-4phenyl)-[3-[*N*-(2-hydroxyethyl)carbazolyl]]diazene obtained for the first time by this research. Both compounds have intermolecular hydrogen bonding abilities due to the polarity of molecules and this is clearly reflected in their melting points (e.g. 78-84°C for *N*-(2-hydroxyethyl) carbazole and 330-333°C for (*N,N*-dimethyl-4-phenyl)-[3-[*N*-(2-hydroxyethyl) carbazolyl]]diazene.

Conclusions

In this study was synthesized a new carbazole derivative (*N,N*-dimethyl-4phenyl)-[3-[*N*-(2-hydroxyethyl) carbazolyl]]diazene which can be used in obtaining of new photorefractive materials. This compound has photoconductive and photorefractive functionality (i.e. *N*-(2-hydroxyethyl)carbazole included in the chemical structure of final product) as well as photochromic group such as azo which can be used in non-linear optical (NLO) field. In this respect the synthesized (*N,N*-dimethyl-4phenyl)-[3-[*N*-(2-hydroxyethyl)carbazolyl]]diazene and

organic intermediate were purified by HPTLC and then each of them were characterized by spectral analyses (e.g. FTIR, and UV-Vis) and Differential Scanning Calorimetry (DSC) as well. The physical properties as well as interfacial interactions of the small and high molecules of the studied compounds adsorbed on the chromium/gold sensor in real time (e.g. $\mu g/cm^2$) for different concentrations were investigated by Quartz Crystal Microbalance (QCM) technique. For small frequency shifts (fig. 4-7) of quartz crystals, the frequency changes are primarily determined by the changes in mass of the analysed compounds. Under such conditions, the changes in frequency and mass are related by the Sauerbrey equation calculated in tables 1 and 2.

References

1.XIE, S., NATANSOHN, A., ROCHON, P., Chem. Mater., 5, 1995, p.403
2.KIPPELEN, B., TAMURA, K., PEYGHAMBARIAN, N., PADIAS, A.B., HALL, H.K. Jr, J. Appl. Phys., 74, 1993, p. 3617
3.TAMURA, K., PADIAS, A.B., HALL, H.K. Jr, PEYGHAMBARIAN, N., Appl. Phys. Lett., 60, 1992, p. 1803
4.NATANSOHN, A., ROCHON, P., Chem. Rev., 102, 2002, p. 4139
5.IONITA, I., ALBU, A.M., RADULESCU, C., MOATER, E.I., Scientific Study & Research., 12, nr. 2, 2011, p.101.
6.MOERNER, W.E., GRUNNET-JEPSEN, A., THOMPSON, C.L., Annual Review of Materials Science, 27, 1997, p. 585.
7.IONITA, I, ALBU, A.M, RADULESCU, C, MOATER, E.I, CIMPOCA, G.V, GIRTU, M, Journal of Optoelectronics and Advanced Materials, 10, nr. 11, 2008, p. 2859.
8.HO, M.S., BARRETT, C., PATERSON, J., ESTEGHAMATIAN, M., NATANSOHN, A., ROCHON, P., Macromolecules, 29, 1996, p.4613.
9.***ASTM-E-2009-02: Standard Test Method for Oxidation Onset Temperature of Hydrocarbons by Differential Scanning Calorimetry
10.***ISO 11357-6: 2008 Plastics - Differential Scanning Calorimetry (DSC) - Part 6: Determination of oxidation induction time (isothermal OIT) and oxidation induction temperature (dynamic OIT)
11.CIMPOCA, G.C., RADULESCU, C., STANCU, A., DULAMA, I.D., LET, D., Quartz Crystal Microbalance. Nanoanalytical Method. Applications, 2009, Ed. Bibliotheca.
12.CIMPOCA, G.V., RADULESCU, C., DULAMA, I.D., POPESCU, I.V, STIHI, C, GHEBOIANU, A, BANCUTA, I, IONITA, I, CIMPOCA, M, CERNICA, I, AIP Conference Proceedings, 1203, 2009, p.409.
13.CIMPOCA, G.V, RADULESCU, C, DULAMA, I.D, POPESCU, I.V, GHEBOIANU, A, BANCUTA, I, CIMPOCA, M, CERNICA, I, STAICU, L, AIP Proceedings, 1203, 2009, p. 160.
14.CIMPOCA G.V, RADULESCU C, POPESCU I.V, DULAMA I.D, IONITA I, CIMPOCA M, CERNICA I, GAVRILA R, AIP Conference Proceedings, 1203, 2009, p.415.
15.CIMPOCA G.V., POPESCU I.V, DULAMA I.D, RADULESCU C, BANCUTA I, CIMPOCA M, CERNICA I, SCHIOPU V, DANILA M, GAVRILA R, IEEE Journal – Proceedings, 1, 2010, p.135.
16.DULAMA I.D, POPESCU I. V, CIMPOCA G.V, RADULESCU C, BUCURICA I.A, BANCUTA I, Journal of Science and Arts, 19, nr. 2, 2012, p.201.
17.DULAMA I.D, POPESCU I.V, CIMPOCA G.V, RADULESCU C, GHEBOIANU A.I, Journal of Science and Arts, 13, nr 2, 2010, p. 341.

Manuscript received: 6.03.2013